International Journal Of
Industrial Electronics Control and Optimization
Print ISSN: 3517-2645
Online ISSN: 3568-2645
Homepage: https://ieco.usb.ac.ir/

Comparison of Dynamic State Estimation Methods in the Time Domain

Saeed Javadi[1] | Ali Hesami Naghshbandy[1] |

Department of Electrical Engineering, University of Kurdistan, Sanandaj, Iran [1]
Corresponding author's email: hesami@uok.ac.ir

Article Info

Article type:
Research Article

Article history:
Received: 5-Mar-2024
Received in revised form: 08-August-2024
Accepted: 09-August-2024
Published online: 21-March-2025

Keywords:
Dynamic state estimation,
Inverter-based resources,
Sample values,
Time domain,.

ABSTRACT

Correct information about a power system's dynamic variables is important and necessary for protection and control issues. Today's power systems, which differ from past systems, face new challenges due to converter-based resources. A solution to these challenges is dynamic state estimation in short time intervals, such as the time domain. This paper simulates a standard 68-bus system in the presence of converter-based resources with a high penetration percentage in DIgSILENT software and compares the performance of four Bayesian filters in estimating the dynamic variables of the synchronous generators of the system using values in the time domain with each other. The four types of filters used include extended Kalman filter, unscented Kalman filter, ensemble Kalman filter, and particle filter. The MATLAB software suite was used for the comparison of the performance of the four filter types in different scenarios, including the presence of measurement and processing noise, extreme noise, network fault, data missing, state estimation time by each filter, and the comparison of time domain method with other methods such as phasor domain. At the end, the advantages and disadvantages of each were identified.

I. Introduction

Today, new power systems, including Converter-Based Resources (CBR) and storage resources, are widespread. With deeper penetration of these sources, the challenges related to the stability, control, and protection of the power system have increased for two crucial reasons: (a) the reduction of system inertia due to the presence of CBRs, and (b) the existence of different time scales from milliseconds or less for CBRs to several minutes or more for synchronous generator boilers. Therefore, it can be mentioned that the high penetration of these sources has caused the new power system to have features such as faster system response, ineffectiveness of common protection logic, and having different power system transients [1, 2]. The following is a review of some works on CBR's presence in power networks.

CBRs in power networks have also affected network distance protection. In [3], adaptive distance protection was used with these CBRs in the condition of fault resistance. As a result, the sensitivity and coordination of distance relays on the transmission lines and the DFIG-based wind farm collector lines were also increased. In [4], the effects of CBRs, such as Double Feed Induction Generators (DFIGs) and Static Series Synchronous Compensator (SSSC), on the stability of power grids were investigated. The system's stability was improved by using a nonlinear controller for these sources.

Today's power systems cannot be properly protected and controlled with these plans due to the random, scattered, and variable nature of renewable energy sources [5].

It has been stated in [1, 6] that in the case without CBR, all network generators are oscillating with respect to a static reference, by using CBRs, the inertia of the whole system is reduced and the reference point also fluctuates, and because other generators also oscillate relative to this (non-static) point, with the presence of CBRs, the fluctuations of waveforms increase. The construction of the phasor by PMUs has a delay due to the use of the DFT algorithm and they cannot follow the fluctuations properly, so we had to use faster units such as

Copyright © A. Hesami Naghshbandy (s).
Publisher: University of Sistan and Baluchestan

MUs that work in the time domain [7].

On the other hand, despite this new power system, it can be stated that dynamic models are widely used for stability, control, and transient studies of power systems [8]. It can be said that the solution to these new power grid challenges should be searched in Dynamic State Estimation (DSE) [9]. DSE can estimate the state of a power system at different scales, so it can be used as a versatile tool to observe the path of the system state [10]. So far, many research works have been conducted on DSE, some of which are mentioned below.

One of the most important state variables in power systems in terms of stability and control is the rotor speed of the synchronous generator, so measuring the rotor speed has always been a fundamental issue. It can be said that estimating the rotor speed without any mechanical connection is a great improvement in the performance of the power system [11]. Researchers in [12] presented the use of DSE based on the Unscented Kalman Filter (UKF) for a nonlinear system connected to an infinite bus with measurable mechanical torque (Tm) and excitation field (Ef) as inputs and used PMUs. In the following, the dynamic states of a system connected to an infinite bus were estimated by considering the transient model (4th-order model) using the Extended Particle Filter (EPF) [13]. In [14], the state variables were estimated by considering the second-order generator using combined DSE methods. A decentralized method was used in [15] to estimate the dynamic state in the power system based on unscented transformation used to estimate the state of the exact equations of the generator, excitation system, and stabilizer. In [16], a novel centralized controller based on the Kalman filter was presented to control multi-input, multi-output industrial processes with heavy interactions and significant time delays and indicated that the controller performed well in tracking the set point and was robust due to changing the system parameters. In [17], the shortcomings of the EKF method, such as the calculation of the Jacobian matrix and the strong dependence on process and processing noises, were stated, and a PSO-EKF was proposed to make an effective re-adhesion estimator. In [18], state estimation was done with a new method called M-estimation. In this work, the robustness of the proposed algorithm was investigated under different conditions, such as incorrect data in the measurement. In [19], the dynamic states were estimated in the presence of non-Gaussian noises with Iterative Extended Kalman Filter methods of the Generalized Maximum similarity type (GM-IEKF). The method was ineffective in the case of large nonlinearities. Next, DSE was done using the UKF estimation method and H-infinity controller, considering uncertainty in the system and the presence of uncertain measurement noise [20]. In [21, 22], non-Gaussian measurement noises and uncertain inputs were considered in the network, and methods such as GM-UKF and EKF were used. In the works that have already been done, various situations, such as communication channel

TABLE I. STRENCHS, WEAKNESSES, ADVANTAGES, AND DISADVANTAGES OF THE PAST WORKS

Reference	Advantages and strengths	Disadvantages and weaknesses
Ref [1, 2]	- Referring to the power system with CBRs and stating its characteristics - Expressing time domain DSE methods - Expressing time domain equations	- Not doing simulation to prove the claim and just reviewing past works
Ref [3-8]	- Applying and modeling CBR resources in the power network - Examining the effects of these resources on challenges, such as stability, control, and network protection - Improving the above challenges by using new methods	- Not using time domain values and using phasor values - Absence of a comprehensive method that can cover all challenges together - The phasor construction algorithms (DFT) used in these references have delays
Ref [9, 10]	- Expressing the characteristics of the power system - Providing a complete description of basic state estimation	- Not considering CBR resources in the investigated power system - Describing static state estimation, which is not applicable to today's power system.
Ref [11-18]	- Estimating state variables of nonlinear systems with EKF and UKF filters - The robustness and convergence of these filters in different scenarios - Developing a PF method and using the EPF method - Using combined state estimation methods to improve other methods - Applying decentralized and centralized DSE methods and comparing them - Using state estimation methods in other engineering sciences [16] - Combining EKF with PSO to improve the performance of EKF [17]	- Using phasor domain values - Using the old power system without the presence of CBRs - Not checking different scenarios in some references - Effectiveness of algorithms for extreme noises - Divergence of state estimation algorithms in some special states, such as non-Gaussian noise - High calculation time due to the use of phasor construction algorithms such as DFT
Ref [19-25]	- Using the EKF and UKF method based on repetition to estimate the parameter and mode for non-Gaussian noises and their robustness - Combining UKF and H-infinity controller in the presence of system uncertainties and non-Gaussian noises - Improving UKF against cyber attacks, innovation errors, and severe nonlinearities - State estimation with a combination of the above methods for non-Gaussian noises - Estimating CBR modes	- Divergence of the above filters in some simulations - Using simple models of synchronous generators like the classic model - Not considering CBR in the studied power systems - Using phasor values (PMU) - Not checking the robustness of some algorithms in scenarios, such as data missing

interruption, high nonlinearity of the system, innovation errors, and bad and incorrect data, have been considered, and filters, such as UKF based on repetition, developed EKF, have been used to estimate the state variables and the parameters of synchronous generators [23-25].

Table I shows a summary of the strengths and weaknesses, as well as the advantages and disadvantages of the references reviewed in Section I.

By studying past works, it can be stated that various methods have been used to estimate the state of the power system, most of which are methods based on the Kalman filter because Kalman filters cover all linear and nonlinear systems and are the best DSE tools.

By stating the above information about the new power system and DSE, it is concluded that DSE has limitedly been used for networks with CBRs, and it is the best tool for protecting, controlling, and monitoring new systems.

So, the innovation of this paper is the use of DSE in the time domain in a centralized manner with Bayesian methods for networks with CBRs with a high penetration level. The above operations are also implemented for different scenarios, and the advantages and disadvantages of each of the filters are specified.

The general structure of the paper is as follows. Section II describes DSE formulation in the time domain, the estimation model, and the discretization process. Section III describes Bayesian filters and how to implement them. Section IV simulates the system and implements the filters on it. Finally, Section V reports simulation results.

II. DSE Formulation

As already mentioned, a typical power system includes synchronous generators and electromechanical transients with a time period of several seconds. This power system also has electromagnetic transients, which are much faster than electromechanical transients and are ignored [1].

With the increasing penetration of CBRs and the effect of those devices in power systems, the system's dynamic response is highly dependent on the dynamic response of the power electronic devices, their control systems, and dynamic issues related to converters [26].

Also, this equipment distorts the network signals and their deviation from the sinusoidal state. It should be mentioned that the time period studied for CBRs is from microsecond to millisecond due to switching in converters. Hence, the result is that common phasor representation is usually useful for electromechanical studies of synchronous generators. It is unsuitable for electromagnetic problems due to the delay in constructing the phasor (discrete Fourier transform process or DFT), so time domain information (sample values) must be used.

A. Representation of Equations in the Time Domain

According to the previous section, the relationships and measurements required for the dynamic estimation equations should be changed.

Regardless of the time scales of different dynamics, the system can be described with the differential and algebraic equations (1) [1].

$$\begin{cases} \dot{x}(t) = f\big(x(t), y(t), u(t), w(t)\big) \\ 0 = g\big(x(t), y(t), u(t), w(t)\big) \end{cases} \tag{1}$$

in which x(t) is the state vector, y(t) is the algebraic state vector, u(t) is the input vector, and f and g are nonlinear functions.

To go to the time domain, the above equations must be converted from continuous to discrete form, which is fully explained in Subsection C. The important point here is that according to [1], to obtain the equations in the time domain after discretization, they will remain unchanged, and the only difference is that the voltage and current signals will no longer be in the phasor state, but they will be sampled in the time domain and determined by the sampling frequency.

B. The Desired Model for Network Generators

This section explains the synchronous generator model considered for state estimation and then states Euler's method for discretization of state equations. In this paper, a sub transient model generator with IEEE-type I exciter and Power System Stabilizer (PSS) are implemented using Eq. (2) [27, 28].

$$\frac{d\delta}{dt} = \omega_0 \Delta\omega \tag{2a}$$

$$\frac{d\Delta\omega}{dt} = \frac{1}{2H}(T_m - T_e - K_D\Delta\omega) \tag{2b}$$

$$\frac{de'_d}{dt} = \frac{1}{T'_{q0}}\Big(-e'_d - \big(x_q - x'_q\big)\Big\{i_q - \frac{\big(x'_q - x''_q\big)}{\big(x'_q - x_{ls}\big)^2}\big(e'_d + \big(x'_q - x_{ls}\big)i_q + \varphi_{2q}\big)\Big\} \tag{2c}$$

$$\frac{de'_q}{dt} = \frac{1}{T'_{d0}}\Big(-e'_q - (x_d - x'_d)\Big\{i_d - \frac{(x'_d - x''_d)}{(x'_d - x_{ls})^2}\Big\}\big(e'_q + (x'_d - x_{ls})i_d + \varphi_{1d}\big)\Big\} + E_{fd} \tag{2d}$$

$$\frac{d\varphi_{1d}}{dt} = \frac{1}{T''_{d0}}\big(e'_q - \big(x'_d - x_{ls}\big)i_d - \varphi_{1d}\big) \tag{2e}$$

$$\frac{d\varphi_{2q}}{dt} = \frac{1}{T''_{q0}}\big(-e'_d - \big(x'_q - x_{ls}\big)i_q - \varphi_{2q}\big) \tag{2f}$$

$$T_E\frac{dE_{fd}}{dt} = -\Big(K_E + S_E\big(E_{fd}\big)\Big)E_{fd} + V_R \tag{2g}$$

$$T_A\frac{dV_R}{dt} = -V_R + K_A R_F - \frac{K_A K_F}{T_F}E_{fd} + K_A(V_{ref} + V_{PSS} - V_t) \tag{2h}$$

$$T_F\frac{dR_F}{dt} = -R_F + \frac{K_F}{T_F}E_{fd} \tag{2i}$$

$$\frac{dV_{WF}}{dt} = -\frac{1}{T_W}V_{WF} + K_{PSS}\frac{\omega_0}{2H}\times \quad (2j)$$
$$((T_m - T_e - K_D\Delta\omega))$$
$$\frac{dV_{PSS}}{dt} = -\frac{1}{T_2}V_{PSS} + \left(\frac{1}{T_2} - \frac{1}{T_w}\frac{T_1}{T_2}\right)V_{WF} + \quad (2k)$$
$$K_{PSS}\frac{T_1}{T_2}\frac{\omega_0}{2H}((T_m - T_e - K_D\Delta\omega))$$

Equations (2a-2f), (2g-2i) and (2j, 2k) are related to the generator, the excitation system, and the PSS, respectively. In these equations, δ is the angle of the rotor, Δω is the deviation of the rotor speed, $\dot{e'_d}$ and $\dot{e'_q}$ are transient voltages of the stator in the direction of d and q axes, φ_{1d} and φ_{2q} are dampers flux in the direction of d and q, E_{fd} is the excitation field, R_F is the scaled output of the stabilizing transformer, V_R is the scaled output of the amplifier, V_{WF} is the output voltage of steady state eliminator filter, V_{PSS} is the PSS output voltage, and i_d and i_q are the stator currents along d and q axes, respectively. The parameter T_m is the mechanical torque, T_e is the electrical torque of the air gap, ω_0 is the nominal value of the angular frequency, H is the inertia, and K_D is the damping coefficient. The parameters T''_{d0}, T''_{q0}, T'_{d0}, T'_{q0}, T_A, T_E, T_F, T_W, T_1, and T_2 are time constants in seconds, K_E, K_F, and K_A are controller gains, and K_{PSS} is the PSS gain. x_d and x_q are the reactances along the d and q axes, x'_d and x'_q are the transient reactances along the d and q axes, respectively. The above equations should be written as (3-8) in order to be in the framework of state equations.

$$\dot{x} = f_c(x,u) + w_c$$
$$y = h_c(x,u) + v_c \quad (3)$$
$$E[w_c w_c^T] = Q \quad (4)$$
$$E[v_c v_c^T] = R \quad (5)$$
$$x = [\delta\ \Delta\omega\ e'_q\ e'_d\ \varphi_{1d}\ \varphi_{2q} E_{fd}\ V_R\ R_F\ V_{WF}\ V_{PSS}]^T \quad (6)$$
$$u = [T_m\ i_R\ i_I\ V_{ref}]^T \quad (7)$$
$$y = [e_R\ e_I]^T \quad (8)$$

in which x is the state vector, u is the input vector, y is the output vector, the functions f_c and h_c represent the state and output equations, respectively, and the index c indicates the continuous state.

The vectors w_c and v_c represent the process and output noises, respectively, which are modeled as Gaussian (with zero means), and their covariance matrix is defined according to Eq. (4) and (5), respectively, where $E[*]$ is the statistical expectation.

In Eq. (7, 8), e_R are e_I the stator voltages along the R and I axes, and i_R and i_I are the stator currents along the R and I axes, respectively.

To convert Eq. (2) to f_c according to Eq. (3), i_d, i_q, and T_e are written as Eq. (9-11) in terms of *x* and *u*.

$$i_d = i_R sin\delta - i_I cos\delta \quad (9)$$
$$i_q = i_I sin\delta + i_R cos\delta \quad (10)$$
$$T_e \approx P_t = (e'_d + i_q x'_q) i_d + (e'_q - i_d x'_d) i_q \quad (11)$$

Similarly, in order to be able in $h_c[*]$ to write e_R and e_I in terms of relations of *x* and *u*, Eq. (12, 13) should be used.

$$e_R = (e'_d + i_q x'_q) sin\delta + (e'_q - i_d x'_d) cos\delta \quad (12)$$
$$e_I = (e'_q - i_d x'_d) sin\delta - (e'_d - i_q x'_q) cos\delta \quad (13)$$

Finally, the state equations are written in terms of state variables and inputs.

C. Discretization of Equations and its Relations

Assuming that the sampling frequency of merging unit (MU) devices, which have the same role in the time domain as the PMU units in the phasor domain, is f_s, and the sampled time interval is equal to $\Delta t_s = \frac{1}{f_s}$, so, as a result, the values of $T_m(j\Delta t)$, $i_R(j\Delta t)$, $i_I(j\Delta t)$, and $V_{ref}(j\Delta t)$ as input and $e_R(j\Delta t)$and $e_I(j\Delta t)$ are output where *j=1,2,...,k*, is applied to the above state equations as the time sample, and the state values of $x = [\delta\ \Delta\omega\ e'_q\ e'_d\ \varphi_{1d}\ \varphi_{2q}\ E_{fd}\ V_R\ R_F\ V_{WF}\ V_{PSS}]^T$ are estimated [1, 27]. For discretization, it should be done as follows, where $j\Delta t_s$ becomes *k*.

In order to make the equations discrete, the definition of the derivative for the variable x is used as described in Eq. (14).

$$\dot{x} = \frac{x(k) - x(k-1)}{\Delta t_s} \rightarrow x(k) = x(k-1) + \dot{x} \times \Delta t_s \quad (14)$$

in which Δt_s is sampling interval and *k* and *k-1* are actually the same as $k\Delta t_s$ and $(k-1)\Delta t_s$.

By placing the above relation in the state matrix relations, Eq. (15) is obtained:

$$x(k) = x(k-1) + \Delta t_s \times (f(x,u) + w_c \quad (15)$$

Finally, by simplifying, Eq. (16) is obtained:

$$x_k = f(x_{k-1}, u_{k-1}) \times \Delta t_s + x_{k-1} + w_{k-1} \quad (16)$$
$$y_k = h(x_k, u_k) + v_k$$

The above equations show those related to the discrete state of a system, which is in the time domain, and phasor values are no longer used, and synchronized sample values are used.

III. An Overview of the Bayesian Filtering Method

Along with many successes in estimating linear systems, Kalman also made achievements for nonlinear systems.

These nonlinear methods include EKF, UKF, EnKF, and PF. The main difference between these methods is how to calculate the mean and covariance of the system states.

In EKF, the state equations of the system are linearized using Taylor expansion to the first approximation, and the mean and covariance are calculated using Jacobian matrices.

In the UKF method, mean and covariance are calculated using sigma points and passing these sigma points from the nonlinear function.

In EnKF, the mean and covariance are extracted using sequential Monte Carlo methods, and the state distribution is created by collecting these particles. In the above methods, it

is assumed that the processing and measurement noise in Gaussian and Bayesian methods are used, but the PF method is not dependent on Gaussian noise, and similar to the EnKF method, particles are used to calculate the possible distribution of state variables [27].

In the Bayesian framework, the above algorithms are implemented similarly. After the initialization, the above filters receive a data sample as input in each stage. Then, two stages of prediction and filtering are performed, and the state variables are estimated. In the prediction stage, the mean and covariance of states at time k are predicted based on the values of time k-1. The predicted values are corrected with the measured values in the filtering stage. The details of the implementation of the filters are fully described below.

A. Extended Kalman Filter (EKF)

The EKF method linearizes the system using Jacobian matrices and includes the following steps [27].

Prediction stage:

In Eq. (17) and (18), the state and covariance matrix of the states are predicted.

$$x_k^- = f(x_{k-1}, u_{k-1}) + w_{k-1} \quad (17)$$

$$P_k^- = F_{k-1} P_{k-1} F_{k-1}^T + Q_d \quad (18)$$

Filtering step:

The updating or filtering stage is defined by Eq. (19-22), respectively.

$$x_k = x_k^- + K_k \tilde{y}_k \quad (19)$$

$$K_k = P_k^- H_k^T (H_k P_k^- H_k^T + R_d)^{-1} \quad (20)$$

$$\tilde{y}_k = z_k - h(x_k^-, u_k) \quad (21)$$

$$P_k = (I - K_k H_k) P_k^- \quad (22)$$

in which x_k^- and P_k^- are the priori values of mean and variance, respectively. They are derived from the values of the previous step, i.e. k-1. The values of x_k and P_k are the posterior values of mean and variance, respectively, which are obtained by adding the measured values of z_k to the previous values. K_k is the gain of the Kalman filter. $\tilde{y}_k$ represents the remainder between $h(x_k^-, u_k)$ and z_k. F_k and H_k are Jacobian matrices expressed by Eq. (23) and (24).

$$F_{k-1} = \left.\frac{\partial f}{\partial x}\right|_{x_k^-, u_{k-1}} \quad (23)$$

$$H_k = \left.\frac{\partial h}{\partial x}\right|_{x_k^-, u_k} \quad (24)$$

B. Unscented Kalman Filter (UKF)

The UKF method is the unscented transformation for taking a set of samples to represent the probability distribution of states and propagating these samples through functions f and g to generate the mean and covariance of states [29]. The UKF method is described as follows:

Prediction stage:

The prediction stage includes Eq. (25-30).

$$x_k^{i-} = f\left(x_{k-1}^i, u_{k-1}\right) + w_{k-1} \quad (25)$$

$$x_{k-1}^0 = x_{k-1} \quad (26)$$

$$x_{k-1}^i = x_{k-1} + \left(\sqrt{(n+\kappa)P_{k-1}}\right)_i \quad i = 1, \dots, n \quad (27)$$

$$x_{k-1}^{i+n} = x_{k-1} - \left(\sqrt{(n+\kappa)P_{k-1}}\right)_i \quad i = 1, \dots, n \quad (28)$$

$$x_k^- = \sum_0^{2n} W_i x_k^{i-} \quad (29)$$

$$P_k^- = \sum_0^{2n} W_i (x_k^{i-} - x_k^-)(x_k^{i-} - x_k^-)^T + Q_d \quad (30)$$

Filtering step:

The filtering stage includes Eq. (31-37).

$$\mathrm{x_k} = \mathrm{x_k^-} + \mathrm{K_k}\tilde{\mathrm{y}}_\mathrm{k} \quad (31)$$

$$\mathrm{K_k} = \mathrm{P_k^-}\mathrm{H_k^T}(\mathrm{H_k}\mathrm{P_k^-}\mathrm{H_k^T} + \mathrm{R_d})^{-1} \quad (32)$$

$$H_k = \sum_0^{2n} W_i \, \tilde{y}_k \tilde{y}_k^T \quad (33)$$

$$\tilde{\mathrm{y}}_\mathrm{k} = \mathrm{z_k} - \mathrm{z_k^-} \quad (34)$$

$$\mathrm{z_k^-} = \sum_0^{2n} W_i \mathrm{z_k^{i-}} \quad (35)$$

$$\mathrm{z_k^{i-}} = \mathrm{h}\left(\mathrm{x_k^{i-}}, \mathrm{u_k}\right) \quad \mathrm{i} = 0, \dots, 2\mathrm{n} \quad (36)$$

$$\mathrm{P_k} = (\mathrm{I} - \mathrm{K_k}\mathrm{H_k})\mathrm{P_k^-} \quad (37)$$

in which x_k^{i-} and W_i represent the values of 2n+1 point and their weights, and κ is the scaling parameter that determines the position of the sigma points.

C. Ensemble Kalman Filter (EnKF)

In the EnKF method, samples are used to extract the probability distribution of the state variables and their covariance, and the algorithm execution steps are as follows [27, 30].

Prediction stage:

The prediction stage includes Eq. (38-41).

$$\mathrm{x_k^{i-}} = \mathrm{f}\left(\mathrm{x_{k-1}^i}, \mathrm{u_{k-1}}\right) + \mathrm{w_{k-1}} \quad (38)$$

$$\mathrm{z_k^{i-}} = \mathrm{h}\left(\mathrm{x_k^{i-}}, \mathrm{u_k}\right) \quad \mathrm{i} = 0, \dots, \mathrm{n_{EnKF}} \quad (39)$$

$$\mathrm{x_k^-} = \frac{1}{\mathrm{n_{EnKF}}} \sum_{\mathrm{i}=1}^{\mathrm{n_{EnKF}}} \mathrm{x_k^{i-}} \quad (40)$$

$$\mathrm{z_k^-} = \frac{1}{\mathrm{n_{EnKF}}} \sum_{i=1}^{\mathrm{n_{EnKF}}} \mathrm{z_k^{i-}} \quad (41)$$

Filtering step:

The filtering stage includes Eq. (42-46).

$$x_k^i = x_k^{i-} + K_k(z_k^i - z_k^{i-}) \quad (42)$$

$$K_k = P_k^- H_k^T (H_k P_k^- H_k^T + R_d)^{-1} \quad (43)$$

$$P_k^- H_k^T = \frac{1}{n_{EnKF}} \sum_{i=1}^{n_{EnKF}} W_i (x_k^{i-} - x_k^-)(z_k^{i-} - z_k^-)^T \quad (44)$$

$$H_k P_k^- H_k^T = \frac{1}{n_{EnKF}} \sum_{i=1}^{n_{EnKF}} W_i \, (z_k^{i-} - z_k^-)(z_k^{i-} - z_k^-)^T \quad (45)$$

$$z_k^i = z_k + v_k^i \quad (46)$$

Here n_{EnKF} is the number of particles. It should be noted that it is no longer necessary to calculate the error covariance

matrix P_K alone.

D. Particle Filter (PF)

The particle filter method, first proposed by Nicholas Metropolis, is suitable for systems with a high degree of nonlinearity. In fact, the particle filter method is resistant to severe nonlinearities while it has a high computational load. This method, also known as sequential Monte Carlo, will be explained further [27, 31].

First, N random state vectors with the initial probability density distribution function P(x0) are generated, which are represented by $x_{0,i}^{+}\,(i=1,..,N)$. Then, for each time step of k, these particles are published from the nonlinear equation of fk, and their value is calculated for the next sample using Eq. (47):

$$x_{k,i}^{-}=f_k(x_{k-1,i}^{+},w_{k-1}^{i}) \quad (i=1,\dots,N) \tag{47}$$

in which w_{k-1}^{i} is the noise of the process and is calculated from the probability distribution of w_k.

After the measurement is received at time k, the relative conditional probability ($P(y_k|x_{k,i}^{-})$) for each particle $x_{k,i}^{-}$ is calculated. This value can be calculated when the noise probability density function (pdf) and the output matrix are known.

For example, if the measurement function is $y_k=h(x_k)+v_k$, then assuming $x_k=x_{k,i}^{-}$ and also the relative probability of q_i is equal to the value of y^*, then q_i is calculated using Eq. (48) as follows:

$$q_i=P\left[(y_k=y^*)\middle|(x_k=x_{k,i}^{-})\right]=P\left[v_k=y^*-h(x_{k,i}^{-})\right] \tag{48}$$

which is equal to:

$$q_i=\frac{1}{(2\pi)^{\frac{m}{2}}|R|^{\frac{1}{2}}}\times exp\left(-\frac{[y^*-h(x_{k,i}^{-})]^T R^{-1}[y^*-h(x_{k,i}^{-})]}{2}\right) \tag{49}$$

For all particles, the relative probability must be calculated and normalized using Eq. (44) so that the sum of probabilities equals one.

$$q_i=\frac{q_i}{\sum_{j=1}^{N}q_j} \tag{50}$$

In the next step, the resampling step is performed to calculate a new set of particles $x_{k,i}^{+}$. This new set of particles is calculated randomly based on q_i. There are different resampling methods. Here, the standard method is used as follows:

i) The random number r is chosen with a uniform distribution between zero and one.

ii) The set of probabilities q_i are calculated such that they are greater than the value of r, i.e., $\sum_{m=1}^{j-1}q_m<r$, but when we reach the data j, the condition $\sum_{m=1}^{j}q_m>r$ is established, the new particles $x_{k,i}^{+}$ will be equal to the set of particles $x_{k,j}^{-}$.

IV. Simulation and State Estimation

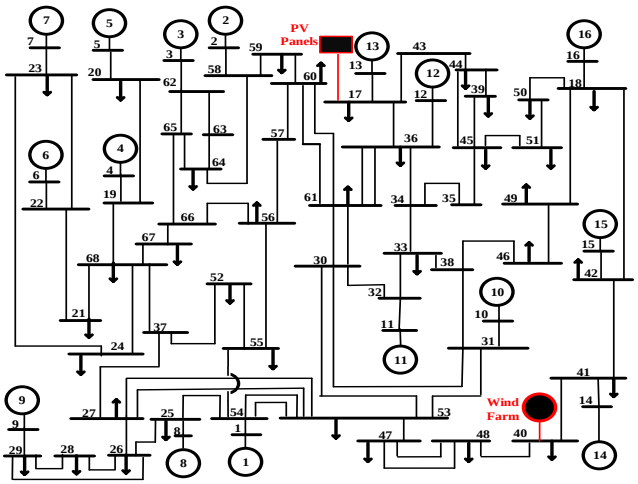


Fig. 1. The 68-bus system simulated in DIGsILENT

This section first describes the simulated system, along with the CBRs. In the following sections, different scenarios are applied in the network, and the above state estimation algorithms are used to estimate the network variables.

A. Simulated System and Results

Fig. 1 is the simulated system in DIgSILNT software, which is the new system of England, New York, and three other geographical regions where the equivalent circuit is available. It has 68 buses, 16 generators, and 83 transmission lines.

It is worth mentioning that the inverter-based resource used in a wind farm includes six two-feed induction generators connected to the 40 bus and a photovoltaic panel connected to the 17 bus. For more information, refer to [31, 32].

The state estimation considered for this article is done centrally and for each generator separately, and the estimated information is sent to the main control center (Fig. 2). Considering that the simulation step must be the same in all generators, the sampling time is also considered to be 1 millisecond.

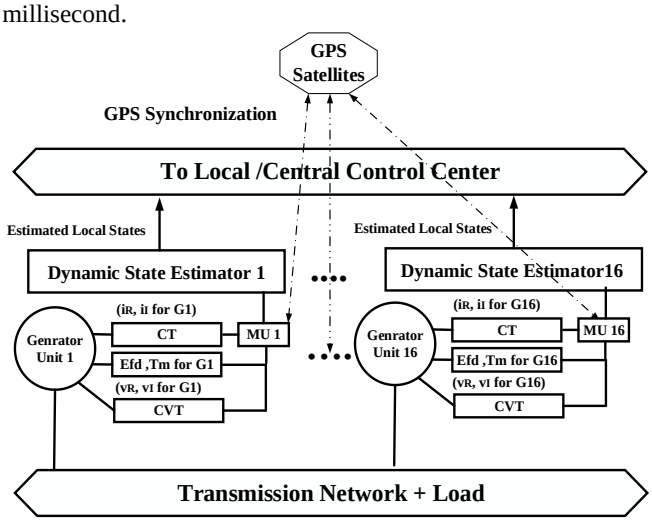


Fig. 2. The estimation of the state of the network in a centralized way

To obtain the initial state of each generator (x_0), the equation $\dot{x} = 0$ in Eq. (2) should be solved for the input values at the initial moment [27].

For all generators, process noise $w_k \sim (0, Q_d)$ with covariance $Q_d = diag([0.0474^2\ 0.0042^2\ 0.0289^2\ 0.0137^2])$ and measurement noise $v_k \sim (0, R_d)$ with covariance $R_d = \text{diag}([0.01^2\ 0.01^2])$ are considered according to [27].

In the following, the simulation results are presented to evaluate the performance of the relationships and the state estimation algorithms of the dynamic variables for the following four scenarios.

B. The First Scenario

In a simple scenario, considering the process and measurement standard noises, the state variables of 16 synchronous generators are estimated.

Figs. 3 to 6 show the state variables estimated by the four filters described in Section III and their actual values related to generator number five (G05). As it is clear from Figs. 3 and 4, in EKF and EnKF filters, after a time of about 2 seconds from the start of state estimation, tend to their real value (black color). The amount of fluctuations and changes for the PF filter (pink color) in the four state variables is less than that of the rest of the filters.

According to Fig. 4, it is clear that the state estimation output for the speed deviation variable tends to its true value, but the amount of changes and the time to reach the true value are more for EKF and EnKF.

It is clear from Figs. 5 and 6 that the amount of changes for UKF and EnKF is more than the others.

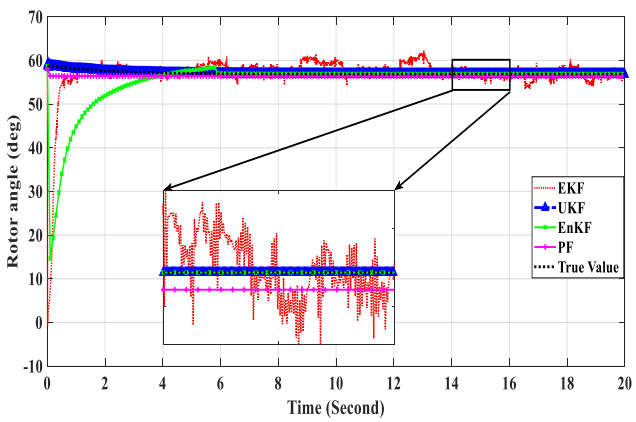


Fig. 3. The dynamic estimation of rotor angle with four studied filters

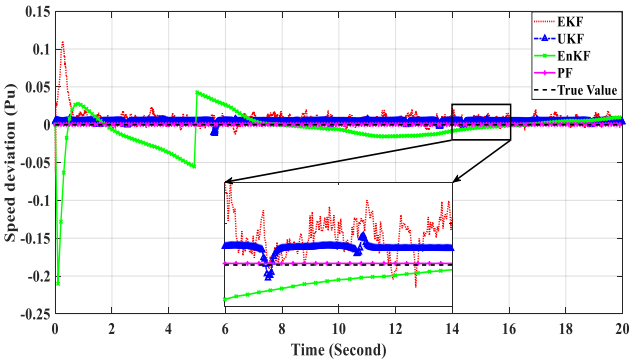


Fig. 4. The dynamic estimation of speed deviation with four studied filters

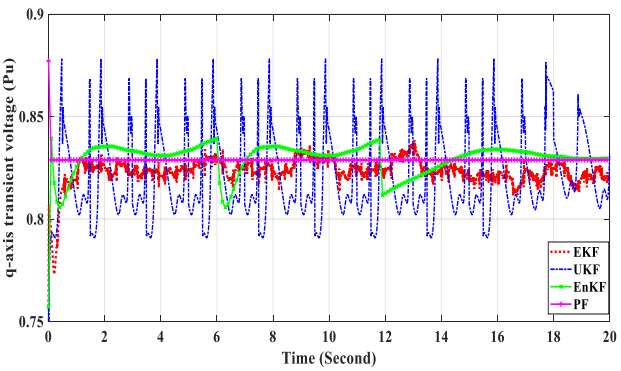


Fig. 5. The dynamic estimation of q-axis transient voltage with four studied filters

In order to show that the state estimation for other synchronous generators works correctly, the maximum deviation index (*MDI*) is defined for some state variables, which is in the form of (51).

$$MDI = max\ |(x_{estimated}(k) - x_{actual}(k)| \quad k = m, m+1, \ldots 20/0.001) \tag{51}$$

in which $x_{estimated}$ is the output state of the estimator, x_{actual} is the actual state of the system, m is the number of samples in that the estimator has reached a stable state, the number 20 is the simulation time, and 0.001 is the sampling interval.

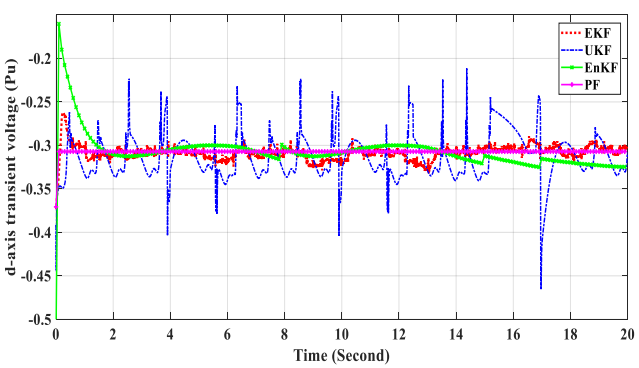


Fig. 6. The dynamic estimation of d-axis transient voltage with four studied filters

TABLE II. COMPARISON OF *MDI* FOR ALL GENERATORS WITH ALL FOUR FILTERS FOR PROCESSING AND MEASUREMENT NOISE

Generator	MDI. EKF	MDI. UKF	MDI. EnKF	MDI. PF
G01	4	5	6.8	2
G02	2.9	4.1	6	1.9
G03	2.8	4.7	5.6	3
G04	4	4.4	6.7	2
G05	3.9	4.1	5.6	2.9
G06	4.1	3.7	6	1.9
G07	4	5.1	5.8	2
G08	3.1	5.2	5.9	2
G09	3.3	5.2	5.1	1.9
G10	3.2	4.1	5	2
G11	3.8	4.2	4.8	2
G12	4	4.3	5	2.7
G13	3.8	4.3	5.3	3.1
G14	3.7	4.1	5.5	3
G15	5.2	3.8	5.8	2.5
G16	4.3	3.4	4.9	2.7

Table II shows the amount of *MDI* for four types of filters after reaching the steady state for the rotor angle variable for 16 synchronous generators. Clearly, the amount of *MDI* for the PF filter is lower than that for other filters.

C. The Second Scenario

In this case, the noise level of the process and measurement is 10 times of the standard noise. In other words, the measuring devices and the system have suffered a severe disturbance, and the first scenario is repeated. Figs. 7 to 10 show the state variables estimated with the four studied filters. It is clear that the noise on the PF filter has almost no effect and causes more changes in other filters for the estimated values compared to the previous states.

It is also clear here that the amount of changes in the estimated values in EKF, EnKF, and UKF is more than the PF filter.

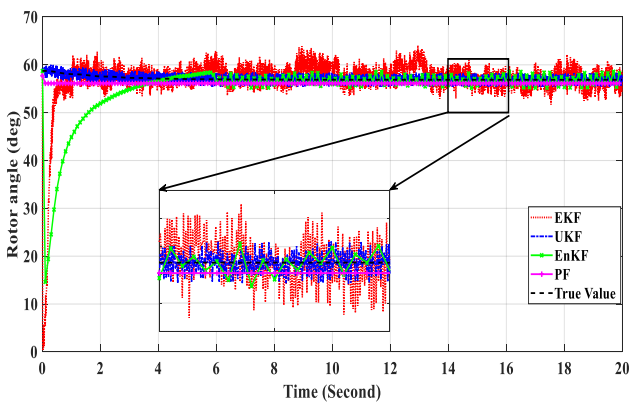


Fig. 7. The dynamic estimation of rotor angle with four studied filters for extreme noise

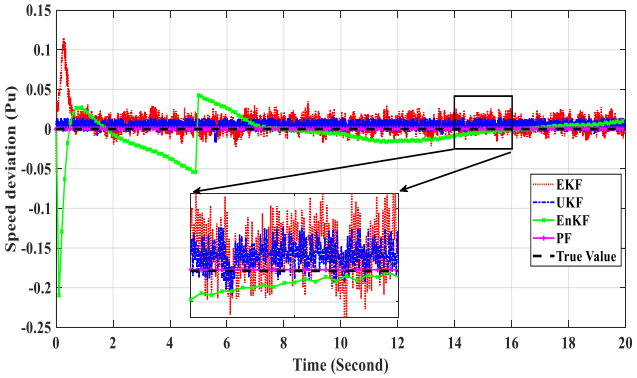


Fig. 8. The dynamic estimation of speed deviation with four studied filters for extreme noise

Figs. 9 and 10 show the transient voltages along the d and q axes for intense noise, respectively.

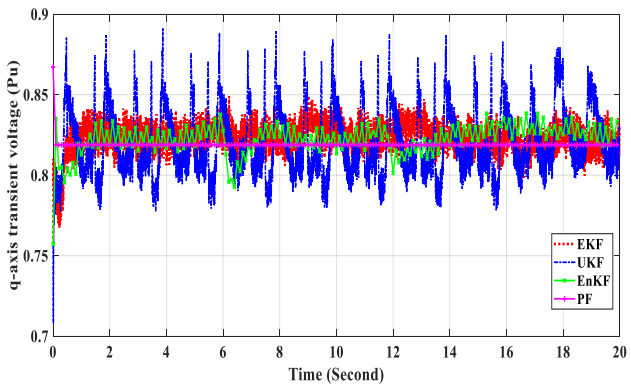


Fig. 9. The dynamic estimation of q-axis transient voltage with four studied filters for extreme noise

Table III shows the amount of *MDI* for all four types of filters after reaching the steady state for the speed deviation variable for 16 synchronous generators. Clearly, the amount of *MDI* for the PF filter is lower than other filters.

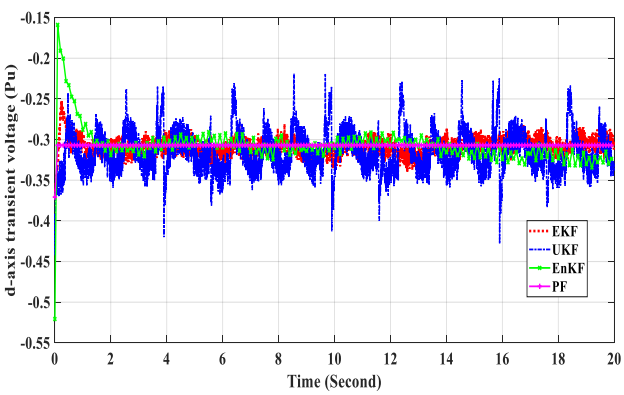


Fig. 10. The dynamic estimation of d-axis transient voltage with four studied filters for extreme noise

TABLE III. COMPARISON OF MDI FOR ALL GENERATORS WITH ALL FOUR FILTERS FOR PROCESSING AND MEASUREMENT EXTREME NOISE

Generator	MDI. EKF	MDI. UKF	MDI. EnKF	MDI. UKF
G01	0.021	0.01	0.02	0.005
G02	0.02	0.011	0.03	0.004
G03	0.019	0.013	0.015	0.008
G04	0.022	0.012	0.018	0.005
G05	0.021	0.011	0.02	0.004
G06	0.023	0.02	0.021	0.004
G07	0.024	0.019	0.021	0.006
G08	0.022	0.02	0.022	0.007
G09	0.022	0.014	0.021	0.006
G10	0.02	0.015	0.02	0.005
G11	0.021	0.02	0.022	0.004
G12	0.018	0.017	0.02	0.005
G13	0.019	0.018	0.019	0.004
G14	0.02	0.021	0.019	0.005
G15	0.025	0.016	0.021	0.005
G16	0.027	0.013	0.02	0.004

D. The Third Scenario

In this scenario, a three-phase fault occurs on line 65-66 in the third second, and after 150 milliseconds, the breakers on both sides of the line open and the fault is cleared. Fig. 11 shows the estimation of the dynamic state of the rotor angle with four types of filters with negligible noise.

As it is clear, changes in the PF filter are less than other filters.

A. The Fourth Scenario with Missing Data

The goal of this scenario is to evaluate all the algorithms when the MU measurements are corrupted by missing data. Missing data may result from temporary communication failures and is often identified via error detection schemes associated with communication protocols.

To model missing data, it is assumed that the amount of measured data has reached zero, the zeroing of this data is detected by telecommunication protocols, and with the detection of missing data, the modified state estimation

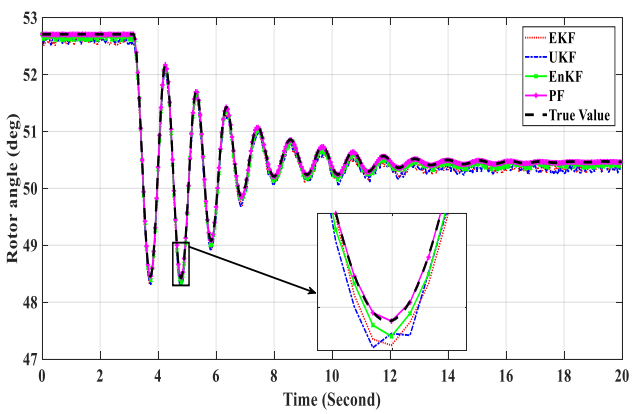


Fig. 11. The dynamic estimation of rotor angle with four studied filters for the three-phase fault on line 13-14

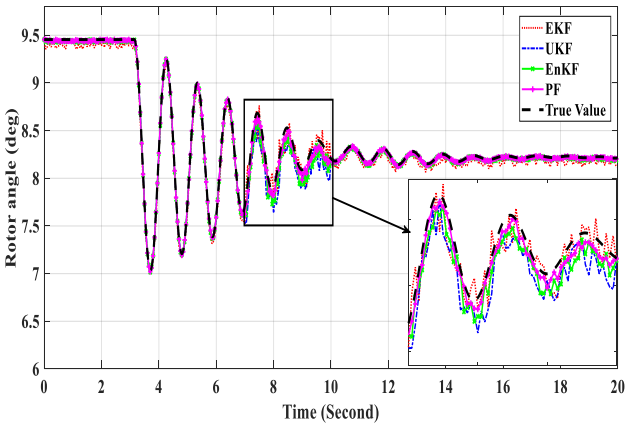


Fig. 12. The dynamic estimation of rotor angle with four studied filters for the data missing in the time of 7 to 8 seconds

algorithm is replaced instead of the original state estimation. As soon as a missing data is detected, the sampling frequency is reduced by about 8 times for higher accuracy, and the pseudo-measurement values obtained by linear interpolation between the samples before and after the event are replaced [27]. In this scenario, the sampling rate is increased from 25 sample/cycle to 200 sample/cycle.

The process noise covariance Q_d is reduced to 1/8 and R_d remains the same as in scenario previous. The. All the other setup remains the same as that in previous scenarios.
The full description of interpolation is given in [27].

To simulate missing data, all measurement data between the 7 to 10 seconds is zeroed.

Fig. 12 shows the estimation of the rotor angle generator one (G01) with the above methods with missing data in 7 to 10 seconds.

As it is clear in Fig.12, with the linear interpolation method, almost all filters are resistant to data missing, and PF filter works better than other filters.

B. The Fifth Scenario

One of the most important issues in DSE is the computation time of each state estimation iteration. For this, the tic command is typed at the beginning of the for loop, and the toc command is typed at the end of the for loop in the MATLAB program. Then, the time obtained is divided by the number of repetitions of the loop, and the execution time of each filter is calculated for one state estimation. Fig. 13 shows the calculation execution time.

As is known, the execution time of the PF and EnKF filters is much longer than that of the EKF and UKF filters, and it is worth mentioning that EKF has the shortest possible time.

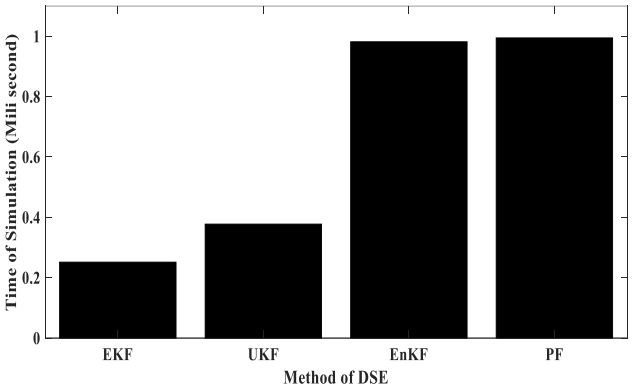


Fig. 13. The computation time of each state estimation iteration

C. The Sixth Scenario

In most previous works, the phasor domain method and PMU have been used for DSE. The purpose of this scenario is to compare the time domain method with the phasor domain method.

In the phasor domain method, the data obtained from the voltage transformer (VT) and current transformer (CT) installed in the generator terminal are first converted into discrete values, and then using the discrete Fourier transform (DFT), the phasor values are extracted from Eq. (52), and these phasor values are used as inputs to state estimation filters.

$$\bar{X} = X_r + jX_i = \frac{\sqrt{2}}{N}\sum_{i=1}^{N}(x_n cos\frac{2n\pi}{N} + jx_n sin\frac{2n\pi}{N}) \quad (52)$$

It should be mentioned that the third scenario (fault on 55-56 line) is repeated in this part.

Fig. 14 shows the performance of four desired filter types with the PMU.

By comparing Figs. 11 and 14 that scenario is the same in both cases, as it is clear, due to the long time of the phasor construction stage by PMU in the phasor method, the accuracy of the phasor method during extreme transients is lower in all filters compared to the time domain method.

By performing this scenario, it is observed that the time domain method performs better in transient states than the previous methods. It should be noted that almost the same results were obtained for other generators.

I. Conclusion

The contribution of this article is the use of DSE algorithms in the time domain with the presence of CBRs, which has not been done in the past. A 68-bus network with CBRs was simulated in the DIgSILNT software. Then, the current and voltage data in the time domain (sample values) related to each generator were extracted with MATLAB software format for six scenarios, including standard noise, extreme noise, network fault, execution time of state estimation, missing data, and comparison with previous methods, and four filters mentioned were implemented on these data. Finally, the related state variables of each generator were estimated. The results are summarized below.

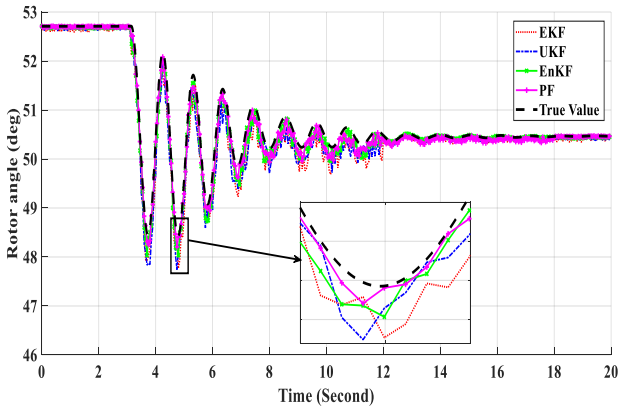


Fig. 14. The performance of four desired filter types with the phasor domain method

Almost all filters detected the state variables correctly, but among them, PF had fewer changes in the steady state of the estimator, and the time to reach the steady state (true state) was shorter. Extreme noise had a lower effect on PF performance. Among the above filters, the duration of PF and EnKF was much longer than that of other filters, which is considered a defect. All filters were resistant to the data-missing scenario, and PF and EnKF performed better than the other filters. The execution time of EKF was shorter than all filters, and it had relatively good performance, which is considered an advantage. Finally, the new DSE was validated by comparing the time domain method and the phasor domain method. The simulations showed that the time domain method performed better in severe transients.

By stating the advantages and disadvantages of each filter and considering the cost required to build each estimator, a balance should be established between these features. For such large networks where CBRs are available, the most favorable filter should be selected by placing MUs in it, so that all state variables related to the generator are properly available.

Future work

What is intended as a new work in the future is the use of state estimation algorithms along with machine learning in distribution and transmission networks.
Another future work is eating is using improved state estimation algorithms.

Another work that can be considered for the continuation of this article is to compare the performance of state estimation methods with control strategies.

REFERENCES

[1] Y. Liu *et al.*, "Dynamic State Estimation for Power System

Control and Protection," *IEEE Transactions on Power Systems*, vol. 36, no. 6, pp. 5909-5921, Nov. 2021.

[2] V. Telukunta, J. Pradhan, A. Agrawal, M. Singh and S. G. Srivani, "Protection challenges under bulk penetration of renewable energy resources in power systems: A review," *CSEE Journal Power Energy Syst.*, vol. 3, no. 4, pp. 365-379, Dec. 2017.

[3] J. Barati, S. Ghodratollah Seifossadat, and M. Joorabian, "Coordination of Adaptive Distance Protection in Transmission and Wind farm Collector Lines under Resistive Fault Conditions," in *International Journal of Industrial Electronics, Control and Optimization*, vol. 3, no. 3, pp. 223-234, July 2020

[4] S. Abazari, "Novel Non-Linear Control of DFIG and SSSC for Stability Increment of Power System," in *International Journal of Industrial Electronics, Control and Optimization*, vol. 7, no. 1, pp. 1-14, March 2024.

[5] N. Hatziargyriou *et al*., "Definition and classification of power system stability revisited & extended,", in *IEEE Transactions on Power Systems*, vol. 36, no. 4, July 2021.

[6] Zhao *et al*., "Power System Dynamic State Estimation: Motivations, Definitions, Methodologies, and Future Work," in *IEEE Transactions on Power Systems*, vol. 34, no. 4, pp. 3188-3198, July 2019.

[7] M. Baechle, V. Knazkins, M. Larsson and P. Korba, "Improved rotor angular speed measurement — A key for proper power grid stabilization," in *2014 IEEE PES General Meeting | Conference & Exposition*, National Harbor, MD, USA, 2014, pp. 1-5.

[8] J. Zhao, *et al*., "Roles of dynamic state estimation in power system modeling, monitoring and operation," in *IEEE Transactions on Power Systems*, 2020.

[9] M. A. Pai, D. P. Sen Gupta, K. R. Padiyar "Small Signal Analysis of Power Systems," in Harrow, U.K: Alpha Science International, 2004.

[10] P. DeRusso, R. Roy, C. Close, A. Desrochers "State Variables for Engineers," 2nd ed. Hoboken, NJ, USA: Wiley, 1998.

[11] C. Wang, Z. Qin, Y. Hou and J. Yan, "Multi-Area Dynamic State Estimation with PMU Measurements by an Equality Constrained Extended Kalman Filter," in *IEEE Transactions on Smart Grid*, vol. 9, no. 2, pp. 900-910, March 2018.

[12] E. Ghahremani, I. Kamwa, "Online state estimation of a synchronous generator using unscented Kalman met phasor measurements units," in *IEEE Transactions on Energy Conversion*, vol. 26, no. 4, pp. 1099-1108, 2011.

[13] N. Zhou, D. Meng and S. Lu, "Estimation of the Dynamic States of Synchronous Machines Using an Extended Particle Filter," in *IEEE Transactions on Power Systems*, vol. 28, no. 4, pp. 4152-4161, Nov. 2013.

[14] L. Lin, Linawati, Lie Jasa and E. Ambikairajah, "A hybrid state estimation scheme for power systems," in *Asia-Pacific Conference on Circuits and Systems*, Denpasar, Indonesia, 2002, pp. 555-558 vol.1.

[15] A. K. Single and B. C. Pal "Decentralized dynamic state estimation in power systems using unscented transformation," in *IEEE Transaction on Power Systems*, vol. 29, no. 2, pp. 794-804, 2014.

[16] H. Fasih, S. Tavakoli, J. Sadeghi and Hamed Torabi, "Kalman Filter-Smoothed Random Walk Based Centralized Controller for Multi-Input Multi-Output Processes," in *International Journal of Industrial Electronics, Control and Optimization*, vol. 2, no. 2, pp. 155-166, April 2019.

[17] R. Havangi, M. Moradi, "PSO-Based EKF Wheel-Rail Adhesion Estimation," in *International Journal of Industrial Electronics, Control and Optimization*, vol. 6, no. 1, pp. 49-62, March 2023.

[18] G. Durgaprasad and S. S. Thakur, "Robust dynamic state estimation of power systems based on M-Estimation and realistic modeling of system dynamics," in *IEEE Transactions on Power Systems*, vol. 13, no. 4, pp. 1331-1336, Nov. 1998.

[19] J. Zhao, M. Netto and L. Mili, "A Robust Iterated Extended Kalman Filter for Power System Dynamic State Estimation," in *IEEE Transactions on Power Systems*, vol. 32, no. 4, pp. 3205-3216, July 2017.

[20] J. Zhao and L. Mili, "A Decentralized H-Infinity Unscented Kalman Filter for Dynamic State Estimation Against Uncertainties," in *IEEE Transactions on Smart Grid*, vol. 10, no. 5, pp. 4870-4880, Sept. 2019.

[21] J. Zhao and L. Mili, "Robust Power System Dynamic State Estimator with Non-Gaussian Measurement Noise: Part II -Theory," arXiv preprint, 1703.04790, 2017.

[22] E. Ghahremani and I. Kamwa, "Dynamic State Estimation in Power System by Applying the Extended Kalman Filter With Unknown Inputs to Phasor Measurements," in *IEEE Transactions on Power Systems*, vol. 26, no. 4, pp. 2556-2566, Nov. 2011.

[23] J. Zhao and L. Mili, "A Framework for Robust Hybrid State Estimation with Unknown Measurement Noise Statistics," in *IEEE Transactions on Industrial Informatics*, vol. 14, no. 5, pp. 1866-1875, May 2018.

[24] A. Rouhani and A. Abur, "Constrained Iterated Unscented Kalman Filter for Dynamic State and Parameter Estimation, " in *IEEE Transactions on Power Systems*, vol. 33, no. 3, pp. 2404-2414, May 2018.

[25] S. A. A. Shahriari, M. Raoofat, M. Dehghani, M. Mohammadi, and M. Saad, "Dynamic state estimation of a permanent magnet synchronous generator-based wind turbine," in *IET Renewable Power Generation*, vol. 10, pp. 1278-1286, 2016.

[26] S. Yu, K. Emami, T. Fernando, H. H. C. Iu and K. P. Wong, "State Estimation of Doubly Fed Induction Generator Wind Turbine in Complex Power Systems," in *IEEE Transactions on Power Systems*, vol. 31, no. 6, pp. 4935-4944, Nov. 2016.

[27] N. Zhou, D. Meng, Z. Huang and G. Welch, "Dynamic State Estimation of a Synchronous Machine Using PMU Data: A Comparative Study, " in *IEEE Transactions on Smart Grid*, vol. 6, no. 1, pp. 450-460, Jan. 2015.

[28] P. Kundur, *Power System Stability and Control* . New York,

NY, USA: McGraw-Hill, 1994.

[29] J. H. Gove, D. Y. Hollinger "Application of a dual unscented Kalman filter for simultaneous state and parameter estimation in problems of surface-atmosphere exchange, " in *JOURNAL OF GEOPHYSICAL RESEARCH*, VOL. 111, D08S07, 2006.

[30] G. Evensen, "Sequential data assimilation with a nonlinear quasigeostrophic model using Monte Carlo methods to forecast error statistics, " in *J. Geophys. Res.*, vol. 99, no. C5, pp. 143–162, May 1994.

[31] G. Anagnostou, L. P. Kunjumuhammed and B. C. Pal, "Dynamic State Estimation for Wind Turbine Models with Unknown Wind Velocity, " in *IEEE Transactions on Power Systems*, vol. 34, no. 5, pp. 3879-3890, Sept. 2019.

[32] S. A. A. Shahriari, M. Raoofat, M. Mohammadi, M. Dehghani, M. Saad, "Dynamic state estimation of a doubly fed induction generator based on a comprehensive nonlinear model," in *Simulation Modelling Practice and Theory*, Volume 69, 2016, Pages 92-112.



Saeed Javadi was born in Kermanshah, Iran. He received his B.E. degree in Electrical Power Engineering from Ilam University, Ilam, Iran, in 2013 and his M.Sc. degree in Electrical Power Engineering from Razi University, Kermanshah, Iran, in 2015. He is currently a Ph.D. student in Electrical Power Engineering at Kurdistan University, Sanandaj, Iran. His current research interests include dynamics, control, and protection of power systems.



Ali Hesami Naghshbandi was born in Sanandaj, Iran. He received his B.S., M.S., and Ph.D. degrees in Electrical Power Engineering from the Iran University of Science & Technology Tehran, Iran, in 1995, 2002, and 2009 respectively. He is currently an Associate Professor at University of Kurdistan, Sanandaj, Iran. His research interests are power system dynamics, stability and control.